



University of HUDDERSFIELD

University of Huddersfield Repository

Papananias, Moschos, Fletcher, Simon, Longstaff, Andrew P. and Forbes, Alistair Barrie

Uncertainty evaluation associated with versatile automated gauging influenced by process variations through design of experiments approach

Original Citation

Papananias, Moschos, Fletcher, Simon, Longstaff, Andrew P. and Forbes, Alistair Barrie (2017) Uncertainty evaluation associated with versatile automated gauging influenced by process variations through design of experiments approach. *Precision Engineering*, 49. pp. 440-455. ISSN 0141-6359

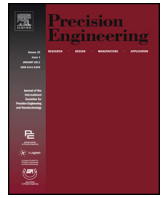
This version is available at <http://eprints.hud.ac.uk/31877/>

The University Repository is a digital collection of the research output of the University, available on Open Access. Copyright and Moral Rights for the items on this site are retained by the individual author and/or other copyright owners. Users may access full items free of charge; copies of full text items generally can be reproduced, displayed or performed and given to third parties in any format or medium for personal research or study, educational or not-for-profit purposes without prior permission or charge, provided:

- The authors, title and full bibliographic details is credited in any copy;
- A hyperlink and/or URL is included for the original metadata page; and
- The content is not changed in any way.

For more information, including our policy and submission procedure, please contact the Repository Team at: E.mailbox@hud.ac.uk.

<http://eprints.hud.ac.uk/>



Uncertainty evaluation associated with versatile automated gauging influenced by process variations through design of experiments approach



Moschos Papananias^{a,*}, Simon Fletcher^a, Andrew Peter Longstaff^a, Alistair Barrie Forbes^b

^a Centre for Precision Technologies, University of Huddersfield, Queensgate, Huddersfield, HD1 3DH, UK

^b National Physical Laboratory, Hampton Road, Teddington, Middlesex, TW11 0LW, UK

ARTICLE INFO

Article history:

Received 29 June 2016

Received in revised form

14 December 2016

Accepted 9 April 2017

Available online 11 April 2017

Keywords:

Versatile automated gauging

Measurement uncertainty

Angular misalignment

Design of experiments

Scanning

Touch-trigger probing

ABSTRACT

Recent advances in versatile automated gauging have enabled accurate geometric tolerance assessment on the shop floor. This paper is concerned with the uncertainty evaluation associated with comparative coordinate measurement using the design of experiments (DOE) approach. It employs the Renishaw Equator which is a software-driven comparative gauge based on the traditional comparison of production parts to a reference master part. The fixturing requirement of each production part to the master part is approximately ± 1 mm for a comparison process with an uncertainty of ± 2 μ m. Therefore, a number of experimental designs are applied with the main focus on the influence of part misalignment from rotation between master and measure coordinate frames on the comparator measurement uncertainty. Other factors considered include measurement mode mainly in scanning and touch-trigger probing (TTP) and alignment procedure used to establish the coordinate reference frame (CRF) with respect to the number of contact points used for each geometric feature measured. The measurement uncertainty analysis of the comparator technique used by the Equator gauge commences with a simple measurement task using a gauge block to evaluate the three-dimensional (3D) uncertainty of length comparative coordinate measurement influenced by an offset by tilt in one direction (two-dimensional angular misalignment). Then, a specific manufactured measurement object is employed so that the comparator measurement uncertainty can be assessed for numerous measurement tasks within a satisfactory range of the working volume of the versatile gauge. Furthermore, in the second case study, different types of part misalignment including both 2D and 3D angular misalignments are applied. The time required for managing the re-mastering process is also examined. A task specific uncertainty evaluation is completed using DOE. Also, investigating the effects of process variations that might be experienced by such a device in workshop environments. It is shown that the comparator measurement uncertainties obtained by all the experiments agree with system features under specified conditions. It is also demonstrated that when the specified conditions are exceeded, the comparator measurement uncertainty is associated with the measurement task, the measurement strategy used, the feature size, and the magnitude and direction of offset angles in relation to the reference axes of the machine. In particular, departures from the specified part fixturing requirement of Equator have a more significant effect on the uncertainty of length measurement in comparator mode and a less significant effect on the diameter measurement uncertainty for the specific Equator and test conditions.

Crown Copyright © 2017 Published by Elsevier Inc. This is an open access article under the CC BY license (<http://creativecommons.org/licenses/by/4.0/>).

1. Introduction

The traditional approach to dimensional inspection on the shop floor is based on hard gauging because coordinate measuring machines (CMMs) require temperature controlled rooms to adequately meet their measurement capability. Certainly there are major differences between manual inspection and automated

* Corresponding author.

E-mail addresses: moschos.papananias@hud.ac.uk (M. Papananias), s.fletcher@hud.ac.uk (S. Fletcher), a.p.longstaff@hud.ac.uk (A.P. Longstaff), alistair.forbes@npl.co.uk (A.B. Forbes).

inspection [1]. Briefly speaking, CMMs are accurate measuring instruments and potentially more versatile and flexible than custom hard gauges. However, they are very costly and require environmental conditions that are unlikely to be met in a shop floor environment. Consequently, this approach proves unsuitable for effective feedback to the production loop. Also, the time required for the inspection cycle can often be longer than the manufacturing cycle itself due to the need to transfer the manufactured parts to the quality control room after the machining process is finished and thermally stabilize them. Dedicated gauging is time consuming and costly, since traceable calibration is required for each hard gauge, and, the repeatability and reproducibility depend on operators. Also, hard gauges require a level of re-engineering when the design of the parts to be measured changes and thus potentially increasing production bottlenecks.

Other types of coordinate measuring systems (CMSs) used in manufacturing include articulated arm coordinate measuring machines (AACMMs), which are manual CMMs. AACMMs are portable and flexible instruments, but they are much less accurate than CMMs [2,3]. As with CMMs, they are also thermally sensitive, though they have a much simpler construction. In addition, unlike automated inspection systems, the manual control of AACMMs adds a non-predictable error source, the operator, and thus producing worse values of repeatability and reproducibility [4].

Although CMMs are one of the most powerful and versatile metrological instruments, the determination of measurement uncertainty of CMMs is not straightforward due to the various influencing factors including both random and systematic effects [5]. However, the influence of systematic effects associated with the CMM can be much reduced in comparator mode in which a machine having high repeatability is required [6,7]. In particular, the substitution method [8], where the CMM is used as a comparator, generally decreases the measurement uncertainty and is used extensively, especially for measurement tasks with high accuracy requirements. In fact, the comparison between the calibrated value of the working standard and the indication of the CMM shows the systematic deviations of the CMM that can be subsequently used to correct the measurement results of production parts. Therefore, the problem of performing an uncertainty budget for comparator measurements is much simpler than CMM measurements [9].

To bridge the gap between CMM measurement and custom hard gauging, automated flexible gauges based on a parallel kinematic structure to ensure high repeatability at fast operating speeds have been recently adopted for process control on the shop floor. Such flexible gauges employ the comparator principle through software to account for the influence of systematic effects associated with the measurement system [6,7]. So, an automated flexible gauge provides all of the automation features of tactile CMMs, but it does so without actually requiring temperature controlled conditions due to the comparator principle. The advantages of the comparator method employed by a CMS are further discussed in Section 3.

The purpose of this work is to study the performance of automated flexible gauge in a shop floor environment using experimental designs. The remainder of the paper is organised as follows. Section 2 presents the background of research concerned with uncertainty evaluation associated with coordinate measurement through experimental designs. Section 3 describes the comparator method for dimensional measurement. Section 4 introduces the automated comparative gauging using a simple measurement task. The fundamental parameter of misalignment is explained and examined along with other important parameters. Section 5 presents the second case study consisted of preliminary and main experiments utilizing a specific manufactured measurement object. Full factorial designs are applied in both case studies to investigate all the possible interactions of the factors through analysis of variance (ANOVA) methods. The measurement results

obtained from both case studies are analysed using Minitab. Finally, concluding remarks are given in Section 6.

2. Background

A large number of research works in the domain of coordinate metrology has been conducted to quantify the measurement accuracy of CMSs such as CMMs and increase it by improvements in hardware, software, and general measurement strategy. In order to ensure that the measurements are accurate, the calibration of the CMM needs to be traceable to the international system of units (SI), in particular, to the international standard of length with known measurement uncertainty [10]. However, CMMs are multi-purpose measuring systems and therefore demonstrating traceability to national standards and, ultimately, to the international standard is not straightforward. Therefore, the only practical way of ensuring that the CMM measurements are accurate is to provide measurement-task-specific traceability statements [10,11]. As a matter of fact, the uncertainty associated with the measurement of a specific feature through a specific measurement strategy is usually referred to as task specific uncertainty. An excellent review for uncertainty sources and methodologies developed to model and assess task specific uncertainty for coordinate measurements is provided by Wilhelm et al. [5]. These authors divided uncertainties associated with CMSs into five main categories: hardware, workpiece, extrinsic factors, sampling strategy, and fitting and evaluation algorithms. Weckenmann and Knauer [12] focused on the last two factors and showed that the way the CMM operator defines the measurement strategy has a strong influence on the CMM measurement uncertainty.

An efficient way to plan and conduct experiments in manufacturing metrology is the method of design of experiments (DOE), which assesses the sensitivity of the measurand to various factors that comprise the measurement process. There is a number of DOE techniques such as factorial designs, response surface designs, Taguchi orthogonal array designs, etc. [13,14]. In manufacturing industry, the most commonly used approach includes factorial designs [15]. Factorial designs fall under two main categories: full factorial designs and fractional factorial designs. Fractional factorial designs are an alternative to full factorial designs when the number of factors is large because they use fewer runs than the full factorial designs. However, only the full factorial designs include all possible combinations of every level of every factor so that all the possible interactions among the factors can be examined. Response surface designs are usually used to refine models after the important factors have been determined using factorial designs [16]. Taguchi orthogonal array design is a type of general fractional factorial design and therefore interactions between the factors are normally not taken into consideration [17,18].

In the reviewed literature, numerous studies have been reported in evaluating the uncertainty associated with coordinate measurement through the DOE method. For example, Barini et al. [19] described a study associated with point-by-point sampling of complex surfaces using a tactile CMM. They carried out a completely randomized full factorial experiment with four factors at two levels each and concluded that the analysis of factorial experiments can help determine the statistically important factors. Similar conclusions, but for length type features of ball bar gauges, were made by Piratelli-Filho and Giacomo [20] who applied a 3^2 factorial design for carrying out a performance test using a ball bar gauge and for investigating CMM errors associated with orientation and length in the work volume. Feng et al. [21] employed a sequential experimentation approach through fractional factorial designs for the measurement uncertainty evaluation of the location of a hole measured by a CMM equipped with a Renishaw TP2 touch-

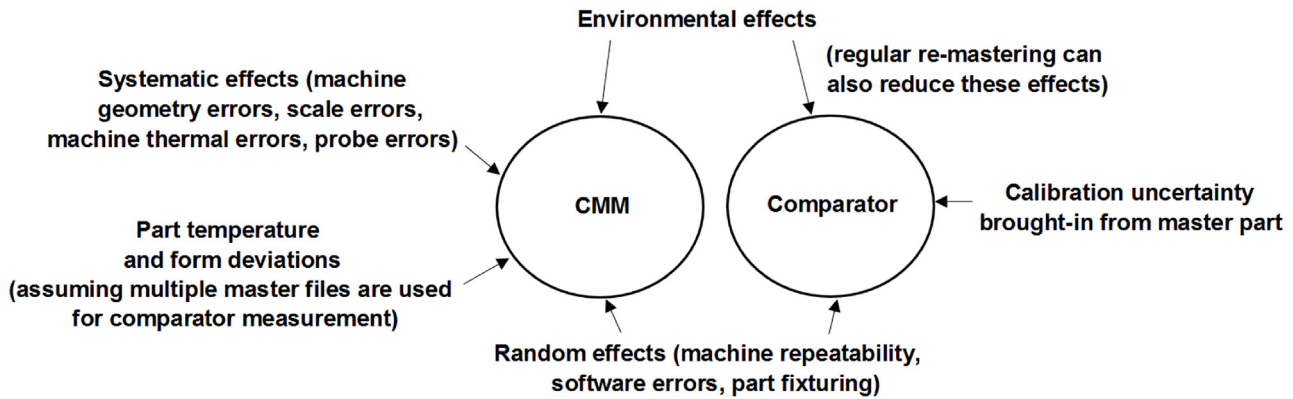


Fig. 1. Measurement uncertainty contributors for CMMs and comparators.

trigger probe. They concluded that, the interaction of speed and probe ratio (the ratio between the diameters of the probe and the ring gauge) is of statistical significance and the uncertainty is minimized when highest speed is used, the stylus length is shortest, and the probe ratio and number of pitch points are largest. Lobato et al. [22] presented a non-fully randomized experimental study due to practical considerations using a CMM located in a temperature controlled room with different levels of room temperature to simulate measurement tasks performed in workshop environments. The factors of interest were: the environment temperature; number of probing points; feature type; probe extension; and stylus length. They concluded that all studied factors were found to be statistically significant as well as the two-factor interactions of environment temperature with feature type, number of probing points with feature type, and probe extension with stylus length.

3. Comparator measurement

The demand in manufacturing for process control on the shop floor has led to many developments in industrial dimensional metrology. One such solution is a software-driven gauging system called Equator, which is used for the case studies in this paper (see Fig. 3). The Equator, developed by Renishaw plc, is an automated flexible gauge that employs the comparator principle through RenCompare software to account for the influence of systematic effects associated with the CMS [6,7]. The Equator machine is constructed with a parallel kinematic constraint mechanism to minimise machine's dynamic errors at high measurement speeds. For handling the temperature effects of the shop floor environment, the re-mastering process can be managed with the built-in sensor and software configuration. Therefore, in comparative coordinate measurement, the main uncertainty contributors can be considered to be: environmental effects, calibrated master part, machine repeatability, part fixturing, sampling strategy, and geometric element best-fit algorithms. Fig. 1 shows the measurement uncertainty contributors for CMMs and comparators.

The principle of operation of the Equator is to gauge or compare data/components. The Equator gauge provides various compare methods, the main ones being “CMM Compare” and “Golden Compare”. In CMM Compare, the calibrated absolute accuracy of the CMM located in a temperature controlled room can be transferred to the shop floor to provide calibrated traceability to Equator measurements. The Golden Compare uses a master part (golden master) to calibrate the Equator and differs from the CMM compare procedure in that there is no requirement to measure the master part on a CMM. The Golden Compare method assumes that the master part is produced at drawing nominal and therefore, any deviation of golden master part to drawing nominals will be included in

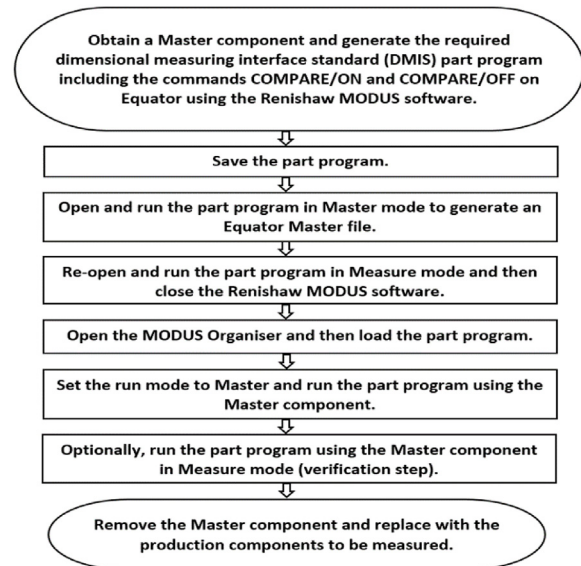


Fig. 2. Golden Compare procedure.

the measurements. However, measurements need to be obtained by traceable measuring systems and therefore, when employing a comparator that uses a production part as a master part, traceability to national standards needs to be established. The Golden Compare procedure consists of the steps shown in Fig. 2.

The methodology for this paper is therefore to conduct a DOE with the factors listed in Fig. 1, excluding the, “calibration uncertainty brought-in from master part.” The reason for this exclusion is that this work studies the performance of the comparator gauge and thus, it concerns only the verification step of the mastering process.

4. Uncertainty associated with length comparative coordinate measurement

In the first stage of this work, a general full factorial design using a gauge block of 100 mm was employed to evaluate the three-dimensional (3D) uncertainty of length comparative coordinate measurement influenced by a two-dimensional (2D) angular misalignment. Gauge blocks are simple mechanical artefacts with accurately known length [23]. The performance of the comparator gauge was evaluated in shop floor conditions at $24^{\circ}\text{C} \pm 0.5^{\circ}\text{C}$ temperatures (uncontrolled temperature conditions) because ideal laboratory conditions do not encompass uncontrollable factors and as a consequence do not represent those conditions in which the

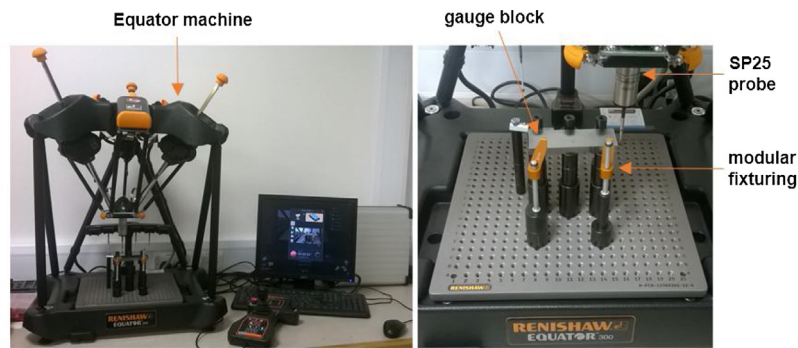


Fig. 3. Test setup on Equator gauge for gauge block inspection.

comparator gauge is likely to be deployed. The stylus used was a typical 21 mm long stylus with stainless steel stem and a 5 mm diameter ruby ball. A general overview of the experimental setup is shown in Fig. 3.

A number of studies have been concerned with the comparison of scanning versus touch-trigger probe measurement in absolute mode [24,25]. However, no prior studies were found that compared scanning and touch-trigger probe measurement in comparator mode. Compared to touch-trigger probing (TTP) systems, scanning probing systems perform faster measurements, gather larger amounts of data, and provide greater coverage of the feature under inspection [26,27]. However, the measurement uncertainty associated with the position of a single point is generally higher in scanning due to dynamic influences [28]. Scanning probing systems can also be used to acquire discrete points, but TTP systems measure discrete points faster than scanning probing systems. Also, in scanning CMMs, machine dynamics limit measurement accuracy at higher speeds. Therefore, conventional scanning probes can achieve measurement accuracy at relatively low scanning speeds where inertial forces are trivial. In fact, while in TTP inertial forces are negligible, in scanning, acceleration and as a consequence inertial loads are always present. In particular, as the machine is moving faster, the accelerations typically increase by the square of scanning speed [29]. For this reason, dynamic compensation measurement techniques have received much attention in recent years [26,29].

The Equator 300 gauge used in this study is a parallel kinematic mechanism-based machine (PKM). Parallel kinematic machines have many advantages over serial structured ones such as improved repeatability and reduced inertial effects at high working speeds [30–32]. This device is supplied with the industry standard SP25 3-axis analogue scanning probe. The SP25 M comprises two sensors in a single housing in order to function either as a scanning probe to gather several hundred surface points each second or as a touch-trigger probe to acquire discrete points on the surface. Therefore, this study sought to investigate the difference obtained in length accuracy between scanning and touch-trigger probe measurement in comparator mode and their impact on measurement uncertainty. In order to investigate the influence of high-speed scanning on the comparator measurement uncertainty, the speed used for scanning was 100 mm/s, which is the maximum recommended for the specific comparator gauge. For TTP, a relative small number of contact points were taken because it was only to evaluate the length of a simple object consisted of two parallel planes of equal sizes, e.g. gauge blocks.

One critical factor affecting CMM performance is the part-alignment procedure used to define the coordinate system or frame of reference (CRF). In addition, estimating the measurement uncertainty contributed by the misalignment of the gauge block depends upon the alignment procedure [33]. While some recommendations for aligning gauge blocks are given in [33], there is no completely

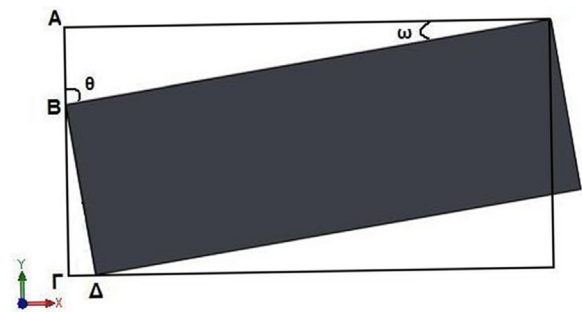


Fig. 4. Angular misalignment of the gauge block.

general method. However, due to the fact that in many practical applications the inspection cycle time is crucial, especially for inspections performed by the Equator which is aimed at medium to high volume gauging, two alignment procedures were chosen to highlight the influence of this factor on the uncertainty of comparator-mode measurement; (1) the non-time-saving alignment in which a relatively large number of discrete points were taken for each geometric feature measured and (2) the time-saving alignment where the number of contact points required for various geometric features was the mathematical minimum.

In coordinate measurement, an improper part fixturing set-up affects measurement accuracy and part throughput. On Equator, when each part is fixtured to within 1 mm relative to the master part, size and position measurements made immediately following re-mastering have a comparison uncertainty, according to the system specification, of $\pm 2 \mu\text{m}$ relative to the certified measurements of the master part. Angular misalignments [34] can largely be avoided by using an appropriate fixture arrangement for part holding. However, holding the parts to be inspected in proper position and orientation is not always an easy task. Also, in some cases, this is not even feasible from a practical point of view e.g. in automated presentation of parts by a robot with limited repeatability or by using a non-repeatable fixturing set-up or both. The alignment error leads to a cosine error [35] ($0.5\gamma L_r$), where γ is the angle between the calculated and actual perpendiculars and L_r the true length of the gauge block, and a first-order error ($\gamma\alpha$), which is negligible for measurement under computer control, since in this case α , which is the perpendicular distance of the projected sensing points from the calculated perpendicular to the surface, can be chosen to be very small [33]. Cosine error is the least of the errors caused by misalignment despite the fact that, this type of error often receives the most attention [36]. Fig. 4 shows the misalignment of the gauge block by tilt along y-axis and Table 1 shows the factors and levels of the gauge block inspection. The length and width of the gauge block are 100 mm and 35 mm, respectively. So, for example, for an angle $\hat{\omega} = 8.627^\circ$ ($AB = 15 \text{ mm}$), the angle $\hat{\theta}$ is equal to 81.373°

Table 1
Factors and levels of the gauge block inspection.

Factors	Levels						
	1	2	3	4	5	6	7
(A) Measurement mode	Scanning	TTP					
(B) CRF	Non-time-saving	Time-saving					
(C) Angular misalignment	a	b	c	d	e	f	g

Table 2
Values for the angular misalignment.

Levels	$\hat{\omega}$	$\hat{\theta}$	AB	$\Gamma\Delta$
a	0.000°	0.000°	0.000 mm	0.000 mm
b	0.573°	89.427°	1.001 mm	0.350 mm
c	1.146°	88.854°	2.000 mm	0.700 mm
d	2.292°	87.708°	4.000 mm	1.400 mm
e	4.014°	85.986°	7.000 mm	2.450 mm
f	5.739°	84.261°	10.000 mm	3.500 mm
g	8.627°	81.373°	15.000 mm	5.250 mm

and therefore, based on Pythagorean theorem, $\Gamma\Delta = 5.25$ mm. In order to investigate if the measurement accuracy degrades as the angle value $\hat{\omega}$ increases, seven levels were used for this factor (see Table 2).

It is worth mentioning that, the use of randomization technique for balancing the effect of extraneous or uncontrollable conditions that can impact the measurement results is not required in this work because the flexible gauge is calibrated when mastering. In addition to that, the present work is designed to be representative of the actual working conditions in which the flexible gauge is used. The Equator comparator has been designed for shop floor gauging with possibly wide temperature variation. Shop floor conditions mostly differ from ideal laboratory conditions in the fact that they have more random and systematic effects. It is usually difficult to distinguish between these effects very clearly [37]. Consequently, the concerns of randomization issues due to practical considerations [22] and/or the need of mixed-effects models [38] in statistical data analyses are largely avoided.

4.1. Measurement uncertainty analysis based on ISO 15530-3

In order to avoid misleading conclusions mainly due to the random effects of shop floor environment and achieve a good level of confidence, the measurement of the gauge block was followed immediately after mastering and repeated ten times without re-mastering so in total, two hundred eighty (280) lengths were determined. For each set of ten repeated measurements, the comparison measurement uncertainty was determined following the uncertainty evaluation methodology given in ISO 15530-3-2011 [8] concerned with substitution measurement. At present, there is no standard specifically concerned with uncertainty evaluation associated with scanning measurement in comparator mode. ISO 15530-3 provides an experimental technique for evaluating uncertainty associated with discrete-point probing. By capturing points by scanning, a high spatial density is achieved. Consequently, through the combination of oversampling and the application of the same measurement routine for master and production parts, the individual probing points are sufficiently coincident to permit the use of this standard for uncertainty evaluation. Therefore, the expanded uncertainty, U , was calculated as follows:

$$U = ku(y) + |\bar{y} - y_{cal}| \tag{1}$$

where k is the coverage factor, $u(y)$ is the standard uncertainty of the mean value of the measurements as assessed below (Formula 2), \bar{y} denotes the mean of the measured values, and y_{cal} is the calibrated or expected value. In such a measurement system, all actual features on the master component are set to their drawing/part program nominal values during the master procedure.

$$u(y) = \frac{\sqrt{\frac{1}{n-1} \sum_{i=1}^n (y_i - \bar{y})^2}}{\sqrt{n}} \tag{2}$$

In order to evaluate the fit of a given distribution (such as the normal in this case) to the data set, a histogram and a normal probability plot of the measurand were produced. However, to easily assess substantive departures from normality, Fig. 5 shows the normal probability plot of the measurand because histograms require more data in order to effectively identify which standard distribution to select. Also, although a probability plot serves a similar

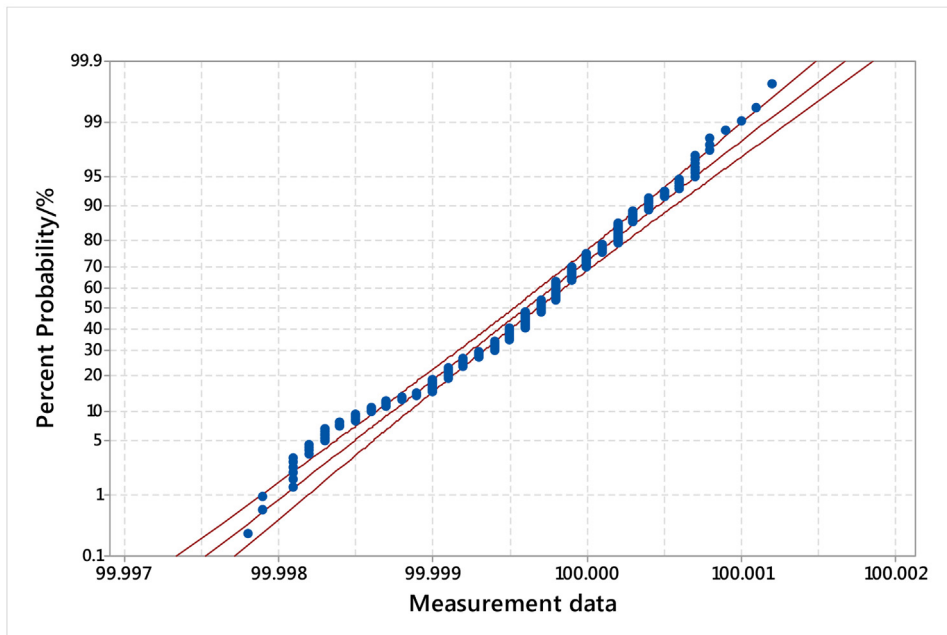


Fig. 5. Normal probability plot of the measured length.

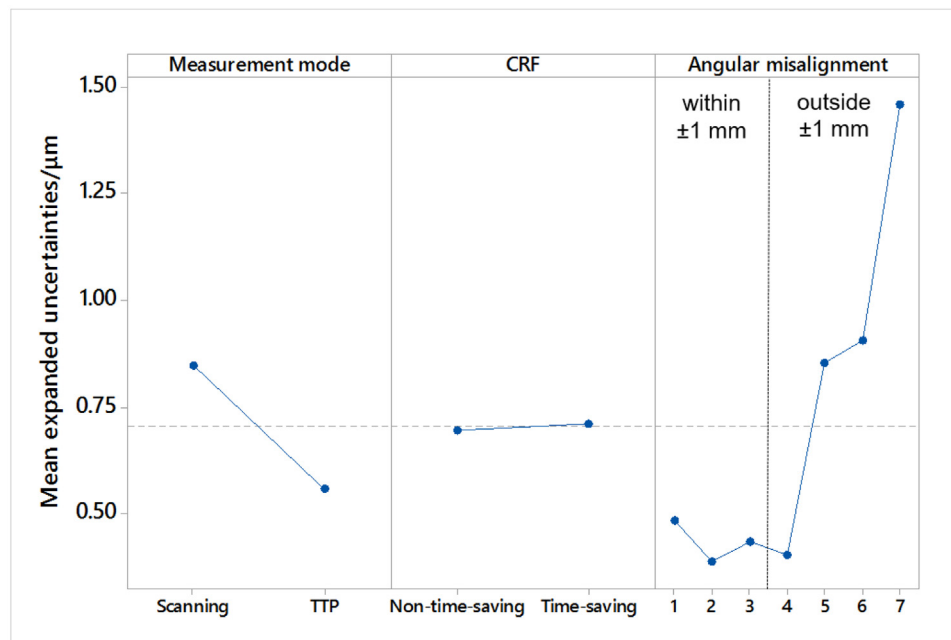


Fig. 6. Main effects plots for expanded measurement uncertainties.

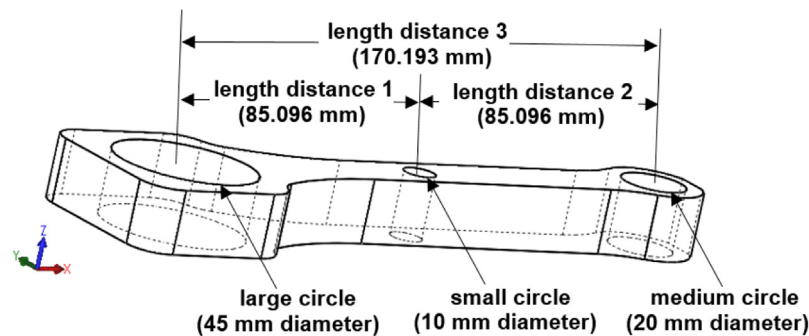


Fig. 7. 3D offset by tilt for the conrod.

function as an empirical cumulative distribution function plot, with a probability plot the distribution fit is easier to be judged by viewing how the data points fall about the line because deviations from the straight line indicate departures from normality.

As can be seen from Fig. 5, the measurement results do follow a normal distribution with negligible departures from normality. For a normal distribution, the interval that contains only one standard deviation provides a confidence level of 68.27%. A confidence level of 95.45% is achieved by using a coverage factor $k=2$ (two standard deviations of the mean) [9]. Fig. 6 shows the main effects plots of the factors for the expanded measurement uncertainties U for $k=2$ and a 95% confidence level.

The results in Fig. 6 show the measurement uncertainty of the comparator technique, which are lower than would be expected from an absolute measurement under workshop conditions. As can be seen, for this measurement task: the comparator measurement uncertainty is smaller in TTP mode than scanning mode (difference in uncertainty between scanning and TTP is less than $0.5 \mu\text{m}$); the number of probing points used to establish the CRF above the mathematical minimum have no statistically significant influence on the comparator measurement uncertainty; and the comparison uncertainty becomes larger as the angular misalignment exceeds

the ± 1 mm fixturing requirement in the Equator specification. As previously stated, this test takes the misalignment well beyond the device's specification. In addition, the interaction plots including all the possible interactions of the factors for the length comparator measurement uncertainties were produced. However, they are very small ($<2 \mu\text{m}$) under all combinations of factors and therefore, factor interactions are shown only for the second experimental design.

Section 4 has provided a guidance procedure for investigating in an effective way the effect of angular misalignment on the comparator measurement uncertainty using simple measurement objects such as gauge blocks. Section 5 follows the same procedure for different measurement tasks on a representative part in order to make an adequate statement about the measurement capability of the flexible gauge using the Golden Compare method. In addition, both 2D and 3D angular misalignments are applied.

5. Comparator measurement uncertainty and advanced misalignment

For the second experimental work, a measurement object (conrod) was designed and then manufactured at the University of

Table 3
Factors and levels of the conrod inspection.

Factors	Levels			
	1	2	3	4
(A) Measurement mode	Scanning 100 mm/s	Scanning 50 mm/s	TTP large number of points	TTP small number of points
(B) CRF	Non-time-saving	Time-saving		
(C) Angular misalignment	0 mm	2.5 mm along z-axis	3 mm along y-axis	3D
(D) Probe configuration	Stylus 21 × 5	Stylus 50 × 5	Stylus 40 × 2	Stylus 30 × 4



Fig. 8. Test setup on Renishaw Equator for preliminary experiments.

Huddersfield's manufacturing facilities so that the uncertainty of comparator-mode measurement can be assessed for different types of measurement within a satisfactory range of the Equator working volume. Therefore, the probe configuration was based on preliminary experiments that involved four different probe configurations, multiple point alignment and minimal point alignment procedures, and measurement mode in scanning and TTP. Also, in order to investigate if a lower speed in scanning and a larger number of contact points in TTP improve or degrade measuring accuracy, two different speeds were used for scanning and two different number of discrete points were selected to be taken for each feature in TTP; one using a relatively large number of contact points and one using a relatively small number of contact points. Then, based on the results of preliminary experiments, angular misalignments were applied with one probe configuration so that the emphasis is on the effects and interactions of angular misalignment with measurement mode and alignment procedure used to define the CRF on the comparator measurement uncertainty. Also, it was argued, if the distribution of points with TTP should follow the same path used for scanning. To avoid the influence of feature form deviations and be able to draw more refined conclusions about the effect of these factors and their interactions on comparator measurement uncertainty, the same path was used for both measurement modes. For an overview of CMM measurement strategies including the selection of the number and distribution of contact points, interested readers are referred to [39].

This paper concentrates on diameter and length measurement. The levels considered for the angular misalignment after mastering were: no offset by tilt in any direction; 2.5 mm offset by tilt along z-axis; 3 mm offset by tilt along y-axis; and the resulting 3D angular misalignment with the simultaneous combination of both (see Fig. 7). Table 3 shows the factors and levels of the conrod inspection.

5.1. Preliminary experiments

A full factorial design was applied to assess the influence of the factors on the comparator measurement uncertainty. The factors of interest in the preliminary experiments were measurement mode, alignment procedure used to establish the CRF, and probe configuration including the following styli: (1) a 21 mm long stylus with stainless steel stem and a 5 mm diameter ruby ball; (2) a 50 mm long stylus with ceramic stem and a 5 mm diameter ruby ball; (3) a 40 mm long stylus with tungsten carbide stem and a 2 mm diameter ruby ball; and 4) a 30 mm long stylus with tungsten carbide stem and a 4 mm diameter ruby ball. The room temperature was set to $20^{\circ}\text{C} \pm 0.5^{\circ}\text{C}$ because choosing the right probe configuration for an inspection process requires the minimization of environmental effects. The measurement of the conrod was followed immediately after mastering and repeated ten times without re-mastering so eighty (80) measurement results were determined for each measurand and for each stylus used. A general overview of the experimental setup is shown in Fig. 8.

5.1.1. Results of preliminary experiments

To illustrate both a measure of central tendency and variability of the data against probe configuration, an interval plot was produced for each measurand. Due to the large number of measurands, only representative figures are presented. Figs. 9 and 10 shows one interval plot for diameter measurement and one interval plot for length measurement.

Based on the interval plots and the associated standard uncertainties for all the measurands, the best results were obtained from the 21×5 and the 40×2 probe stylus. However, the 21×5 probe stylus was selected for the main experiment because a short straight stem configuration is more rigid and generally provides better results. The longer stylus with ceramic stem provided mea-

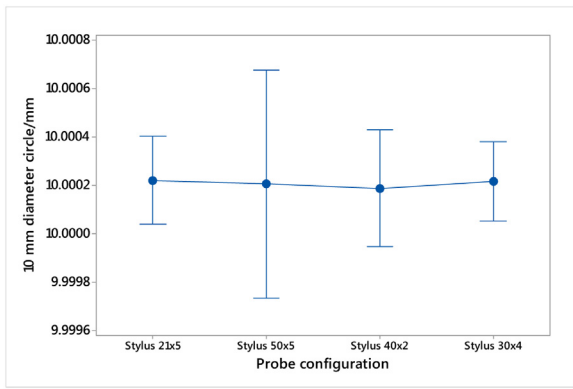


Fig. 9. Diameter of small circle versus probe configuration.

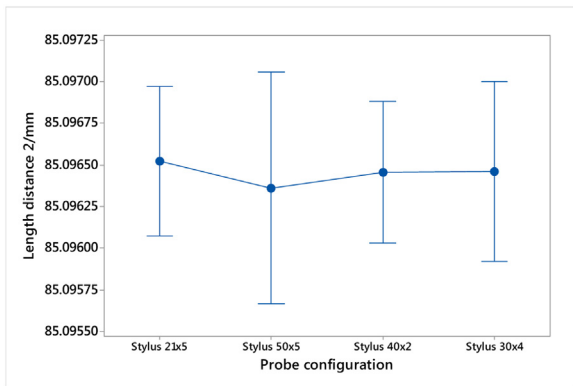


Fig. 10. Length distance 2 versus probe configuration.

surement data having the highest standard deviation and the least probable estimate of the true mean value, while the 30 × 4 probe stylus provided results with higher uncertainties in comparison to that obtained by the 21 × 5/40 × 2 probe styli.

5.2. Main experiment

A full factorial design was applied for the main experiment using the first stylus and involving the factors: measurement mode, alignment procedure used to establish the CRF, and angular misalignment (part misalignment from rotation between master and measure CRFs). After mastering, ten repeated measurements were performed without re-mastering so three hundred twenty (320) measurement results were determined for each measurand.

Furthermore, temperature readings were recorded during the main experiment to record the temperature variation of shop floor conditions. One temperature sensor was used for the ambient temperature, three for the temperature of the machine, and four for the part. This is because, although the flexible gauge is insensitive to ambient temperature changes due to the comparator principle,

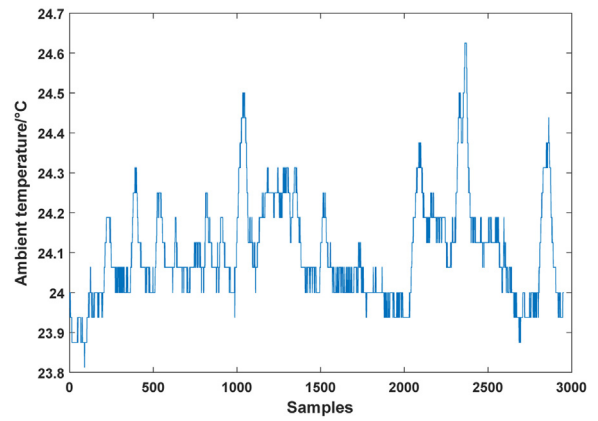


Fig. 11. Sample of ambient temperature.

the accuracy of inspection results is dependent on the influence of temperature on the parts to be measured, unless the flexible gauge has been calibrated using a master part having the same temperature with that of production parts or multiple master files have been used. The part is made of aluminium, which is a material with high thermal conductivity and sensitive to temperature gradients and thus quickly adjusting its temperature to that of the environment. In addition, in the case of manual loading of parts into the machine, the temperature distribution on the part is dependent on operator. Fig. 11 shows a representative sample of the ambient temperature under which the experiment took place (temperature readings were taken every ten seconds).

The fixturing arrangement was slightly modified in order to attach the temperature sensors on the bottom plane of the part. It is also worth mentioning that, an important contribution to the overall measurement uncertainty may owe to the fixturing variability due to the simple fixture arrangement used so that the angular misalignments can be easily applied. However, this is taken into account by the uncertainty contribution associated with the measurement procedure and shall not be considered separately.

5.2.1. Results of main experiment

As with the gauge block inspection, for each set of ten repeated measurements, the comparison measurement uncertainty was determined following the uncertainty evaluation methodology given in ISO 15530-3-2011 [8]. For each measurand, a normal probability plot was produced for assessing substantive departures from normality and all judged to be satisfactory. Table 4 shows the results obtained by the ANOVA procedure based on a least squares regression approach.

Based on the ANOVA results, the statistically significant factors and second order factor interactions for 95% confidence level (p -values < 0.05) are: measurement mode (A) for the small circle; angular misalignment (C) for length distance 1 and 3; and measurement mode (A) and angular misalignment (C) for length distance 2. Note that, R^2 is the percentage of the response variable variation

Table 4
ANOVA results.

Measurands	A p-values	B	C	A*B	A*C	B*C	R ²
Small circle diameter	0.040	0.528	0.729	0.733	0.975	0.768	68.05%
Medium circle diameter	0.052	0.183	0.116	0.305	0.381	0.336	81.81%
Large circle diameter	0.923	0.536	0.087	0.493	0.368	0.709	73.76%
Length distance 1	0.853	0.222	0.013	0.498	0.481	0.449	80.20%
Length distance 2	0.043	0.178	0.000	0.088	0.154	0.147	92.13%
Length distance 3	0.253	0.448	0.000	0.297	0.582	0.707	90.11%

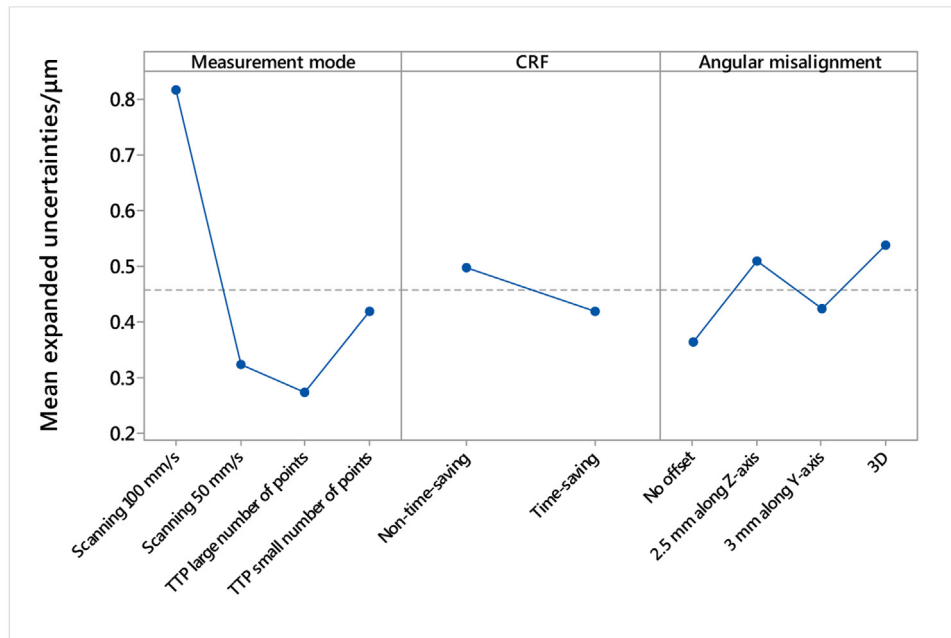


Fig. 12. Main effects plots for the measurement uncertainties of diameter of small circle.

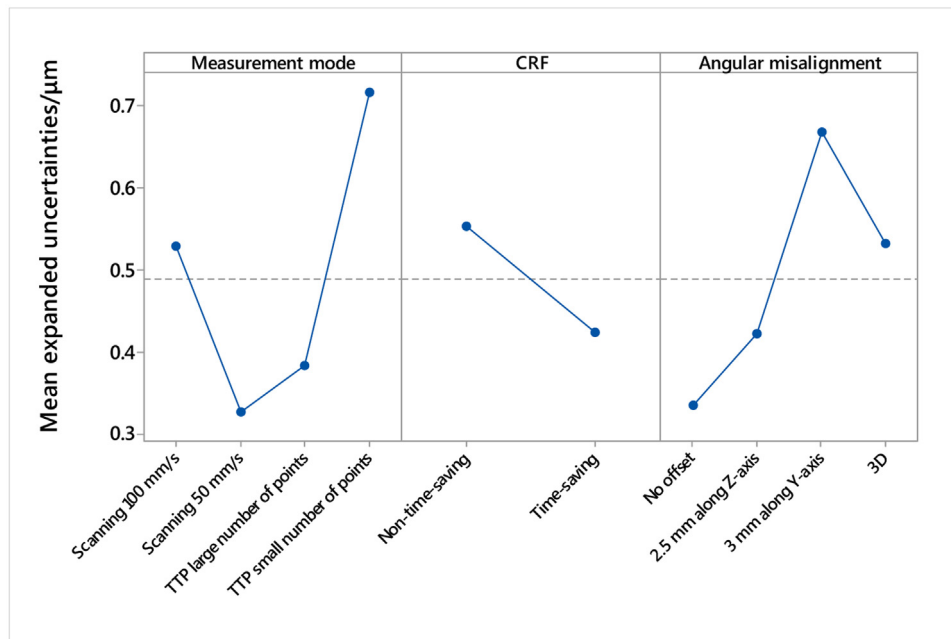


Fig. 13. Main effects plots for the measurement uncertainties of diameter of medium circle.

that is explained by the regression model. Figs. 12–17 show the main effects plots for the expanded measurement uncertainties U for $k=2$ and a confidence level of 95%.

Based on the main effects plots shown in Figs. 12–17, the following conclusions can be made for the specific flexible gauge and test conditions:

1. The comparator measurement uncertainty is not significantly influenced by a time-saving alignment procedure so a considerable saving of time can be achieved by performing a quick alignment procedure without increasing uncertainty. However,

datum uncertainties have to be taken into account for features which are evaluated with respect to datums such as true position and profile [40].

2. Careful consideration needs to be paid for the scanning speed used for the inspection of each feature because this is proportional to the traversed radius. As a consequence, a very high scanning speed will result in increasing the comparator measurement uncertainty (see Figs. 12 and 13 and Figs. 15–17). However, a typical Cartesian CMM without compensation techniques normally requires lower scanning speeds to meet its measurement capability and thus, such low uncertainty values.

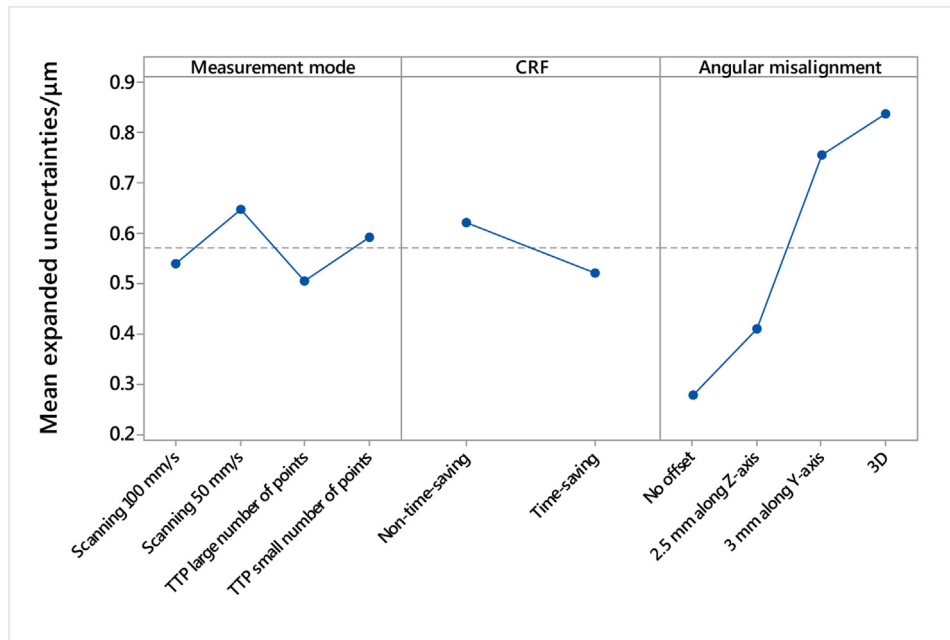


Fig. 14. Main effects plots for the measurement uncertainties of diameter of large circle.

3. A relatively large number of contact points provides smaller measurement uncertainties in comparison to limited sampling (see Figs. 12–14 and Figs. 16 and 17).
4. The difference in comparator measurement uncertainty between scanning and TTP measurement is associated with the scanning speed used for scanning and the number of probing points used for TTP for a given feature, but was found to be less than $1 \mu\text{m}$.
5. The diameter measurement uncertainties remain below $\pm 2 \mu\text{m}$ even when exceeding the specified conditions.
6. The length measurement uncertainties remain below $\pm 2 \mu\text{m}$ under specified conditions and when exceeding the specified conditions only along z-axis for this experimental setup.

Departures from the specified part fixturing requirement of flexible gauge show that the comparator measurement uncertainty is associated with the measurement task, feature size, measurement strategy used, and magnitude and direction of offset angles in relation to the reference axes of the machine.

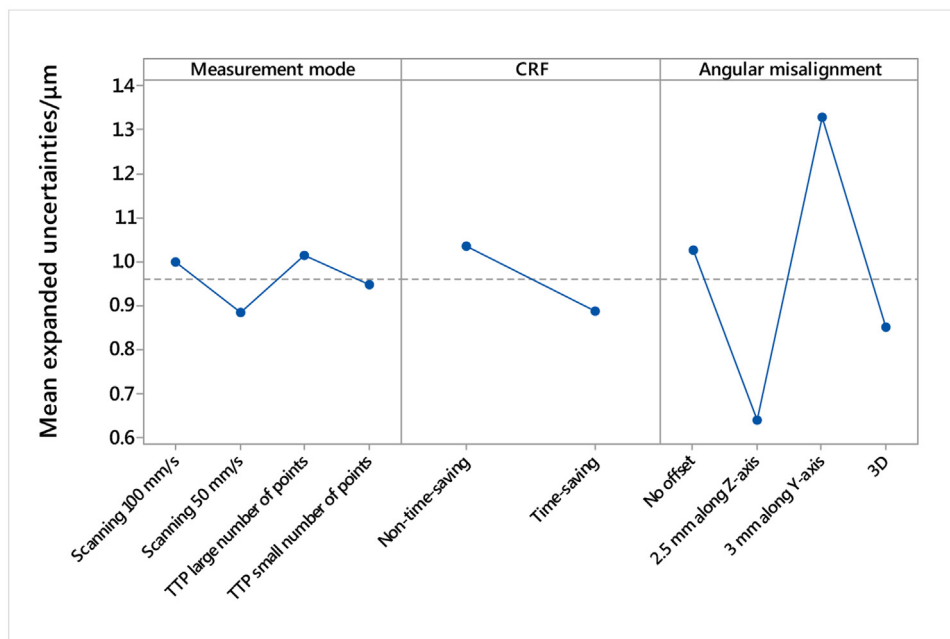


Fig. 15. Main effects plots for the measurement uncertainties of length distance 1.

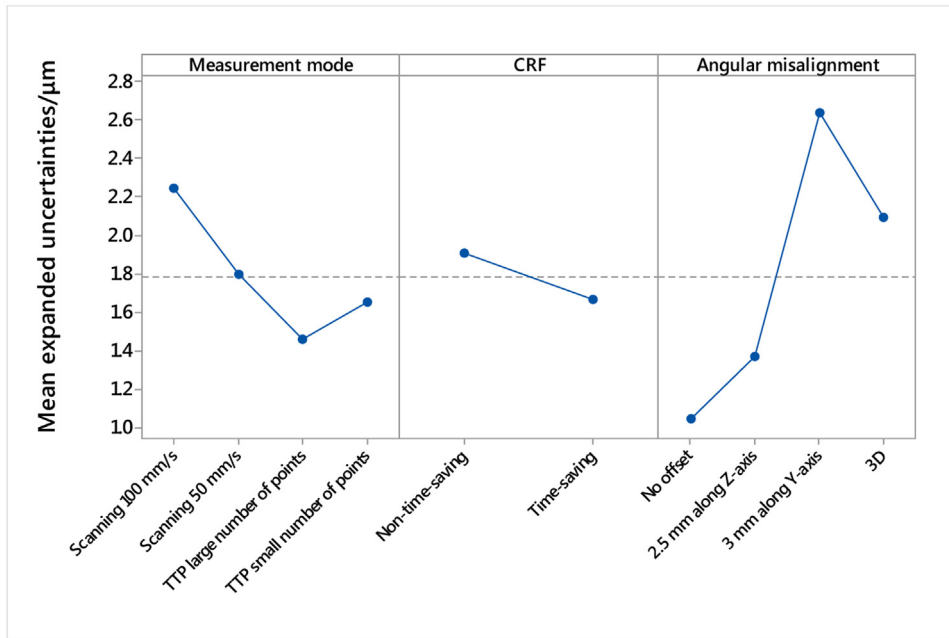


Fig. 16. Main effects plots for the measurement uncertainties of length distance 2.

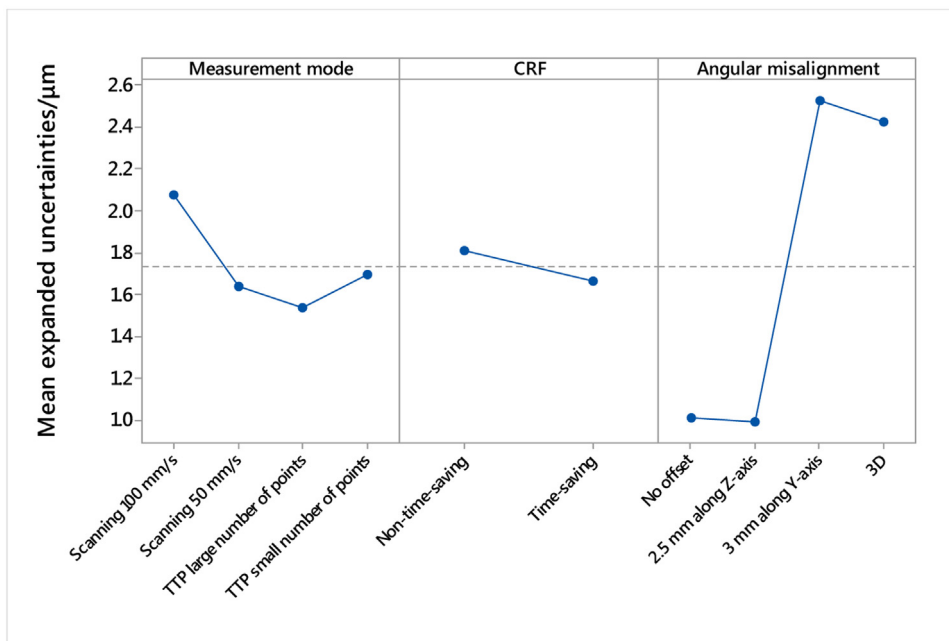


Fig. 17. Main effects plots for the measurement uncertainties of length distance 3.

In addition, the interaction plots including all the possible interactions of the factors for the expanded uncertainties of all six studied measurands were produced. However, only representative results that exceeded the specified comparison uncertainty of the versatile gauge are shown. For example, Figs. 18 and 19 show the factor interactions at the 95% confidence interval for the expanded measurement uncertainties of length distance 3.

Based on the interaction plots shown in Figs. 18 and 19, it can be concluded that the degree of interaction is high only when the misalignment includes a 3 mm offset by tilt along y-axis, which exceeds to a great extent the specified conditions of the system.

5.3. Management of the re-mastering process

Another DOE was employed to examine the time required for managing the re-mastering process in shop floor conditions. The factors were temperature in different values for two different cases as explained later and measurement mode in both scanning speeds used previously for the main experiment (100 mm/s and 50 mm/s). In the first case, the comparator gauge was used to measure the circular features of the part ten times at both scanning speeds immediately after mastering for each different temperature value (21.5 °C, 24 °C, 26.5 °C, and 29 °C). In the second case, the compara-

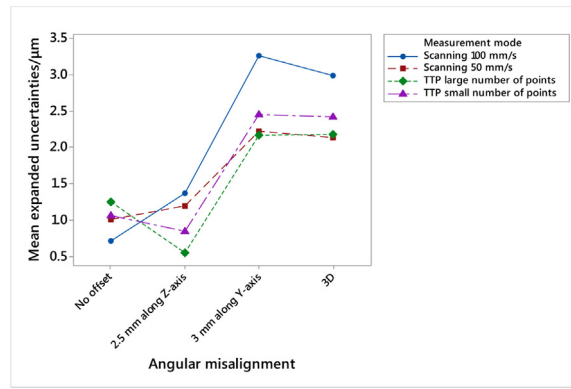


Fig. 18. The interaction plot of measurement mode and angular misalignment for the expanded uncertainties of length distance 3.

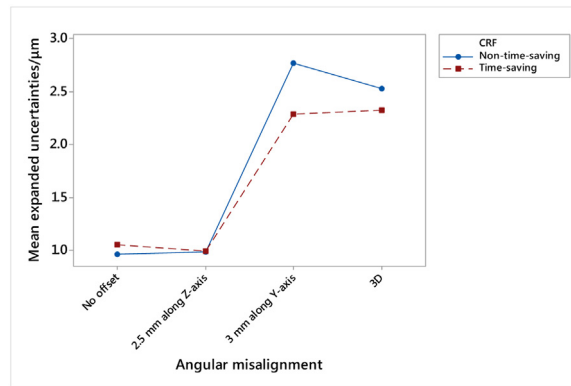


Fig. 19. The interaction plot of CRF and angular misalignment for the expanded uncertainties of length distance 3.

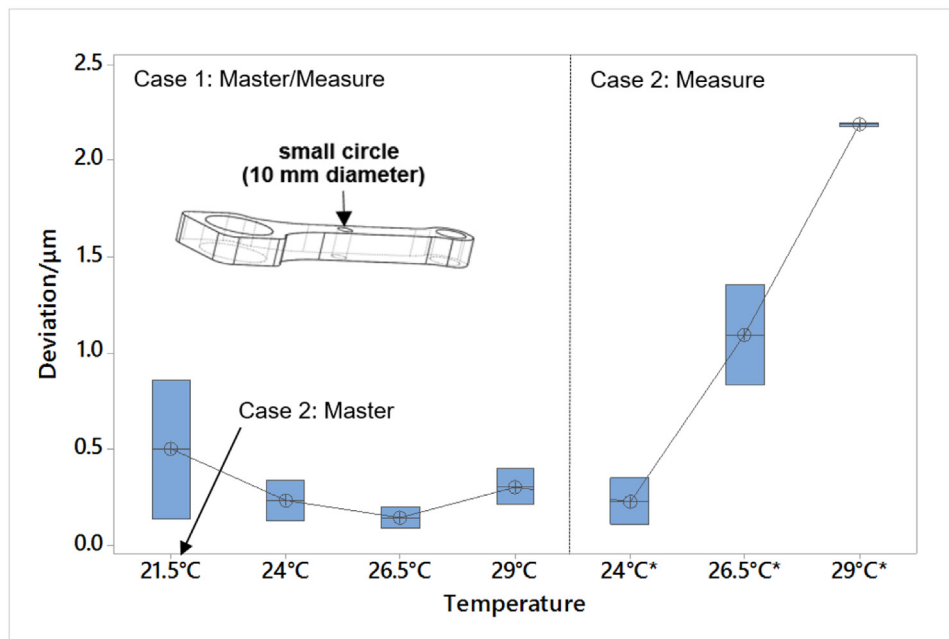


Fig. 20. Boxplot of the diameter of small circle.

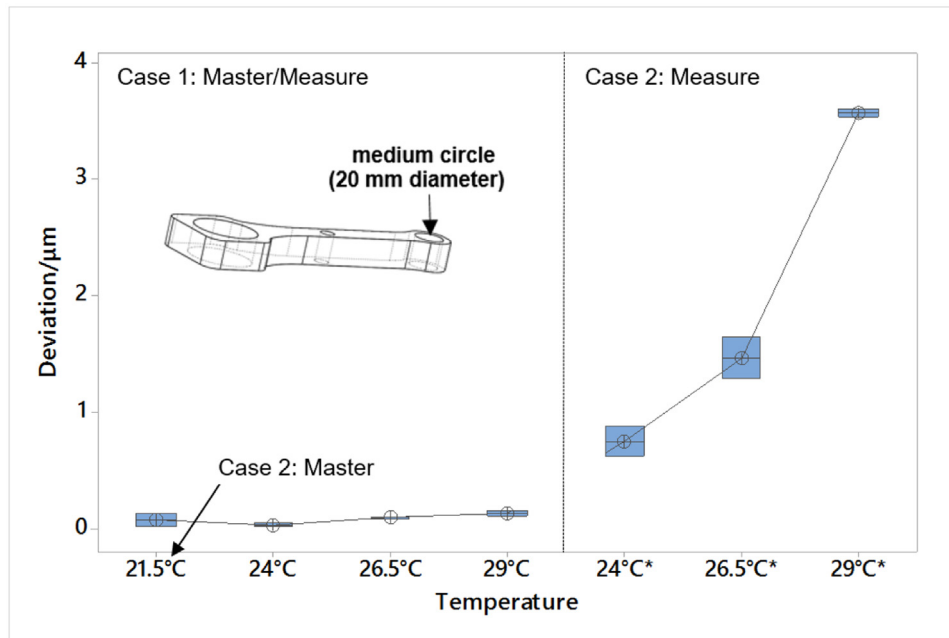


Fig. 21. Boxplot of the diameter of medium circle.

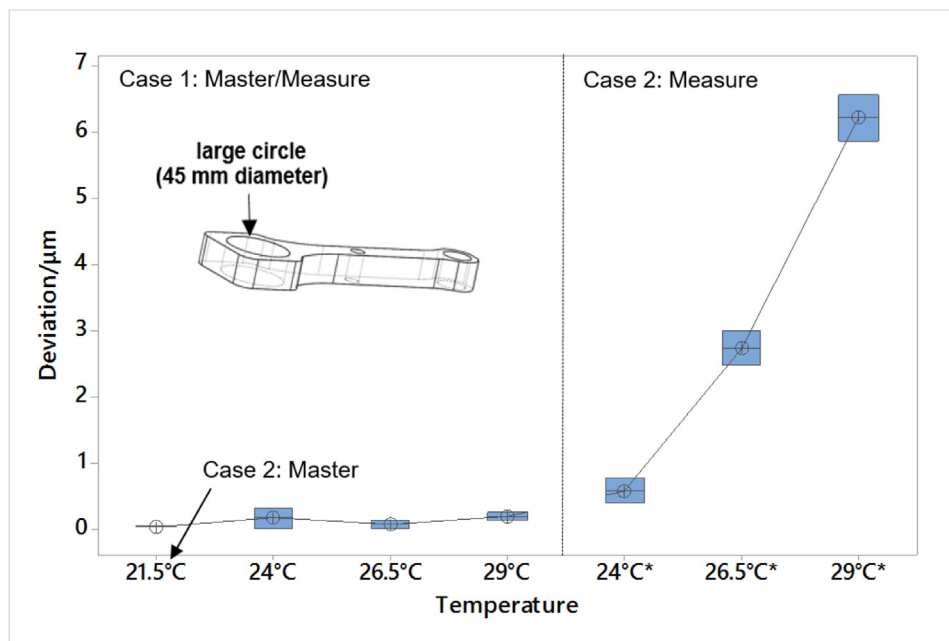


Fig. 22. Boxplot of the diameter of large circle.

tor gauge was mastered at $21.5^{\circ}\text{C} \pm 0.5^{\circ}\text{C}$ and then employed to measure the circular features of the part ten times at both scanning speeds without re-mastering in each case (24°C^* , 26.5°C^* , and 29°C^*). The results obtained from this experimental design are shown in Figs. 20–25.

As shown in Figs. 20–25, the accuracy requirements of the application will determine the time of re-mastering. For highly accurate measurements, the effect of environmental conditions on the comparative measurement can be managed by setting a more restricted upper and lower temperature drift limit by means of built-in sensor feature of Equator. Finally, it is important to note that in Fig. 20, the large data variability owes to the high scanning speeds used for measuring the small circle of 10 mm diameter. However, based on

the results, it can be concluded that a PKM-based flexible gauge is capable of performing fast and accurate measurements.

6. Conclusions

Over the last decades, serious attention has been paid to ensure fast and precise dimensional control on the shop floor with automated inspection systems capable of being integrated into the manufacturing process for in-process feedback to minimize scrap levels. Using this method, it becomes possible to reduce manufacturing costs and increase part throughput. Therefore, this research work has been concerned with such a new process control methodology that involves an adjustable variable gauge based on the

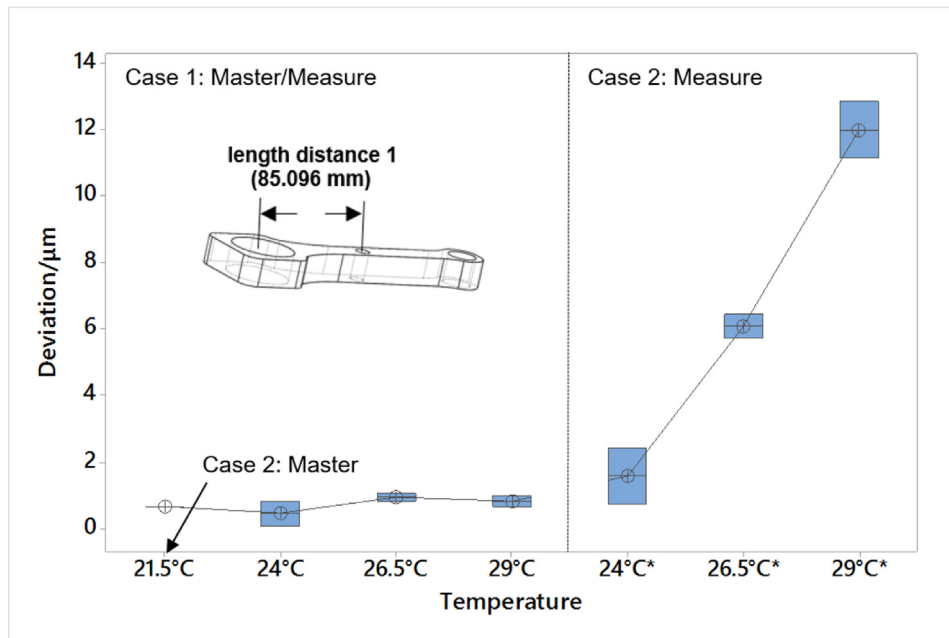


Fig. 23. Boxplot of the length distance 1.

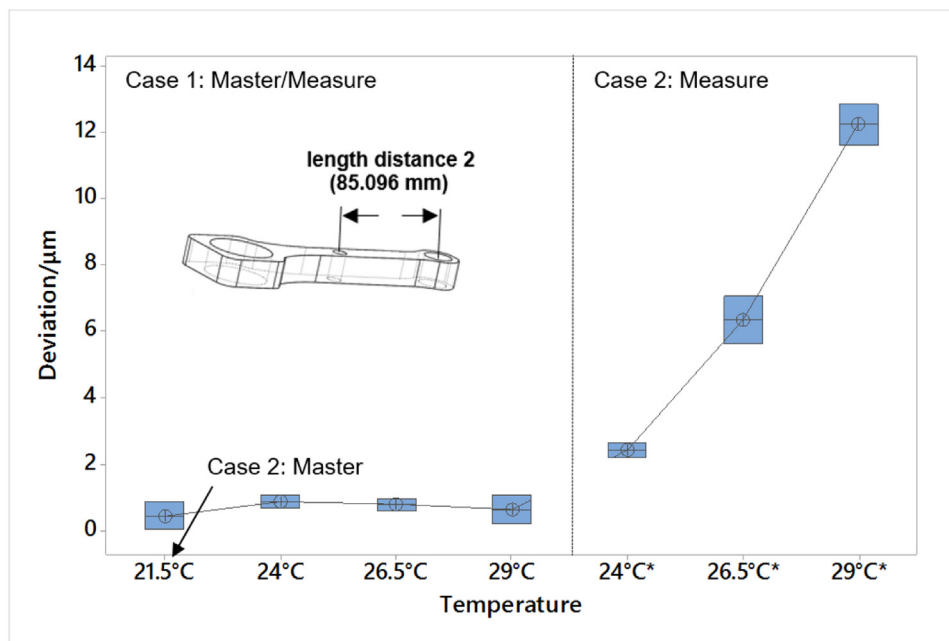


Fig. 24. Boxplot of the length distance 2.

traditional comparison of production parts to a reference master part.

There are practical applications in which fixture arrangements are restricted to set-ups of low repeatability, thus inducing errors in the measurement process. For this reason, full factorial designs have been employed to evaluate the influence of 2D and 3D angular misalignments between master and measure coordinate frames on the comparator measurement uncertainty. It has been demonstrated that for this PKM-based flexible gauge and test conditions there is no significant effect on system repeatability associated with diameter measurement in comparator mode even when the fixturing requirement is exceeded by the studied misalignment values. In particular, it is associated with the feature size, measurement strat-

egy used, and magnitude and direction of offset angles in relation to the reference axes of the machine. However, for length measurement, fixtures/components should relocate within the versatile gauge's volume to an approximate tolerance of ± 1 mm (fixturing requirement according to the system specification) to ensure a successful comparison process. The comparator measurement uncertainty is dependent on the number of probing points used to measure each feature in TTP mode and on the scanning speed used in scanning mode, but not on the number of probing points taken for establishing the CRF. Lastly, the accuracy requirements of the application and task specific uncertainty evaluation are required for managing the re-mastering process.

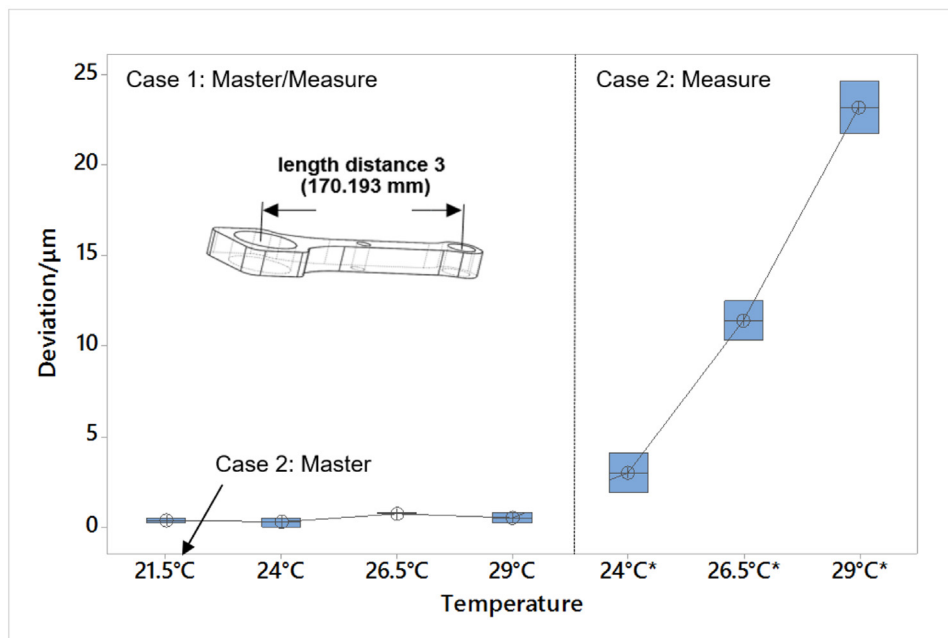


Fig. 25. Boxplot of the length distance 3.

Acknowledgements

The authors gratefully acknowledge the UK's Engineering and Physical Sciences Research Council (EPSRC) funding of the EPSRC Centre for Innovative Manufacturing in Advanced Metrology (Grant Ref: EP/I033424/1) and industrial partners Renishaw PLC for their support throughout this project.

References

- [1] Groover MP. Automation, production systems, and computer-integrated manufacturing. 3rd ed. 2007: Prentice Hall Press; 2017.
- [2] Zhang G. Non-cartesian coordinate measuring systems. *Coord Meas Mach Syst* 2011;467–514.
- [3] Phillips S. Performance evaluation. *Coord Meas Mach Syst* 2011;183–272.
- [4] González-Madruga D, Cuesta E, Barreiro J, Fernandez-Abia AI. Application of a force sensor to improve the reliability of measurement with articulated arm coordinate measuring machines. *Sensors* 2013;13:10430–48.
- [5] Wilhelm R, Hocken R, Schwenke H. Task specific uncertainty in coordinate measurement. *CIRP Ann-Manuf Technol* 2001;50:553–63.
- [6] Forbes AB, Mengot A, Jonas K. Uncertainty associated with coordinate measurement in comparator mode. In: Blunt L, Hansen HN, editors. *Laser Metrology and Machine Performance XI, LAMDAMAP*. Huddersfield, UK: euspen; 2015. p. 150–9.
- [7] Forbes AB, Papananias M, Longstaff AP, Fletcher S, Mengot A, Jonas K. Developments in automated flexible gauging and the uncertainty associated with comparative coordinate measurement. In: Bointon P, Leach R, Southon N, editors. *16th international conference of the european society for precision engineering and nanotechnology*. Nottingham, UK: euspen; 2016. p. 111–2.
- [8] ISO. ISO 15530-3: Geometrical product specifications (GPS) – Coordinate measuring machines (CMM): Technique for determining the uncertainty of measurement – Part 3: Use of calibrated workpieces or measurement standards. Geneva: International Organization for Standardization; 2011. p. 2011.
- [9] JCGM. JCGM 100:2008 Evaluation of measurement data – Guide to the expression of uncertainty in measurement (GUM:1995).: Joint Committee for Guides in Metrology, 2008.
- [10] Swyt DA, Hocken RJ. The international standard of length. *Coord Meas Mach Syst* 2011;31–40.
- [11] Swyt DA. Length and dimensional measurements at NIST. *J Res Natl Inst Standards Technol* 2001;106: 1.
- [12] Weckenmann A, Knauer M, Kunzmann H. The influence of measurement strategy on the uncertainty of CMM-Measurements. *CIRP Ann – Manuf Technol* 1998;47:451–4.
- [13] Box GE, Hunter JS, Hunter WG. *Statistics for experimenters: design, innovation, and discovery*. New York: Wiley-Interscience; 2005.
- [14] Montgomery DC. *Introduction to statistical quality control*. 2007: John Wiley & Sons; 2017.
- [15] Antony J. *Design of experiments for engineers and scientists*. Elsevier; 2014.
- [16] Anderson-Cook CM, Borror CM, Montgomery DC. Response surface design evaluation and comparison. *J Stat Plann Inference* 2009;139:629–41.
- [17] Box G, Bisgaard S, Fung C. An explanation and critique of Taguchi's contributions to quality engineering. *Qual Reliab Eng Int* 1988;4:123–31.
- [18] Li Y, Chen W, Ding J, Wu S. Orthogonal robust design method for product quality innovation management. 2009 ICIM'09 International Conference on: IEEE 2009:120–3.
- [19] Barini EM, Tosello G, De Chiffre L. Uncertainty analysis of point-by-point sampling complex surfaces using touch probe CMMs: DOE for complex surfaces verification with CMM. *Precis Eng* 2010;34:16–21.
- [20] Piratelli-Filho A, Di Giacomo B. CMM uncertainty analysis with factorial design. *Precis Eng* 2003;27:283–8.
- [21] Feng C-X, Saal AL, Salsbury JG, Ness AR, Lin GCS. Design and analysis of experiments in CMM measurement uncertainty study. *Precis Eng* 2007;31:94–101.
- [22] Lobato H, Ferri C, Faraway J, Orchard N. Uncertainty due to experimental conditions in co-ordinate measuring machines. *Proc Inst Mech Eng Part B: J Eng Manuf* 2009;223:499–509.
- [23] Doiron T, Beers J. *The gauge block handbook*. NIST Monogr 2005;180:1–143.
- [24] Ollison TE, Ulmer JM, McElroy R. Coordinate measurement technology: a comparison of scanning versus touch trigger probe data capture. *Int J Eng Res Innov* 2012;4:60–7.
- [25] Puertas I, Pérez CL, Salcedo D, León J, Luri R, Fuertes J. Precision study of a coordinate measuring machine using several contact probes. *Procedia Eng* 2013;63:547–55.
- [26] Pereira P, Hocken R. Characterization and compensation of dynamic errors of a scanning coordinate measuring machine. *Precis Eng* 2007;31:22–32.
- [27] Flack D. *Measurement Good Practice Guide No. 43: CMM Probing*. London, UK: National Physical Laboratory; 2001.
- [28] Weckenmann A, Hoffmann J. Probing systems for coordinate measuring machines. RJ hocken, PH, pereira. *Coord Meas Mach Syst* 2011:93–124.
- [29] Renishaw. *Technical note: The dynamics of co-ordinate measuring machines (CMMs)*. United Kingdom: Renishaw plc; 2003.
- [30] Hertz R, Hughes P. Kinematic analysis of a general double-tripod parallel manipulator. *Mech Mach Theory* 1998;33:683–96.
- [31] Chen J-S, Hsu W-Y. Design and analysis of a tripod machine tool with an integrated Cartesian guiding and metrology mechanism. *Precis Eng* 2004;28:46–57.
- [32] Bi ZM, Jin Y. Kinematic modeling of Exechon parallel kinematic machine. *Robot Comput-Integr Manuf* 2011;27:186–93.
- [33] BS. BS 6808-3: 1989 Coordinate measuring machines – Part 3: Code of practice. UK: British Standards Institution; 1989.
- [34] Farago FT, Curtis MA. *Handbook of dimensional measurement*. 4th ed. United States of America: Industrial Press Inc.; 2007.
- [35] BS. BS 6808-1: 1987 Coordinate measuring machines – Part 1: Glossary of terms. UK: British Standards Institution; 1987.

- [36] Dotson C. Fundamentals of dimensional metrology. 5th ed. 2015: Cengage Learning; 2017.
- [37] Ding H, Scott PJ, Jiang X. A criterion for comparing measurement results and determining conformity with specifications. *Procedia CIRP* 2015;27:143–8.
- [38] Pinheiro J, Bates D. Mixed-effects models in S and S-PLUS. Springer Science & Business Media; 2006.
- [39] Flack D. CMM measurement strategies NPL measurement good practice guide No. 41. NPL-Crown ISSN 2001.
- [40] Pereira PH, Hocken RJ. Measurement uncertainty for coordinate measuring systems. *Coord Meas Mach Syst* 2016;2011:371–86.